LOCALLY RESONANT SONIC CRYSTAL BARRIER FOR LOW FREQUENCY NOISE CONTROL

Samaneh M.B. Fard, Nicole Kessissoglou and Herwig Peters

School of Mechanical and Manufacturing Engineering
UNSW Australia, Sydney NSW 2052, Australia
Email: fardsmb@gmail.com
Email: n.kessissoglou@unsw.edu.au

Abstract

Sonic crystals are periodic arrangements of sound scatterers in a homogeneous fluid medium, where there exists a large impedance mismatch between the scatterers and fluid. Sonic crystals are receiving recent interest as noise barriers for reduction of road traffic noise. The use of a sonic crystal noise barrier is particularly attractive for difficult-to-address low frequency traffic noise sources. In addition to the potential to design sonic crystal barriers to target specific frequency ranges, another benefit in their use is that they allow the free flow of air, thus reducing the effect of wind loading on barriers. The acoustic performance of sonic crystals can be enhanced by replacing the scatterers with locally resonant elements. This paper examines the acoustic performance of a periodic array of rigid perforated cylindrical shells as a potential noise barrier. A parametric study to investigate the effect of the number and size of the perforations on the sonic crystal barrier insertion loss is presented.

1. Introduction

Sonic crystals are periodic arrays of scatterers that are currently being investigated for use as noise barriers using either vertical or horizontal cylinders to represent the scatterers [1-5]. Compared to traditional noise barriers, sonic crystals allow air to pass freely through the structure, thus reducing the effect of wind loading on barriers. Furthermore, a sonic crystal barrier may use less material than traditional noise barriers due to a reduction in filling fraction (volume occupied by the scattering material with respect to the total volume). A notable feature of sonic crystals is the occurrence of high levels of noise attenuation in certain frequency ranges known as band gaps. Varying the distance between adjacent scatterers and increasing the filling fraction are two approaches to improve the acoustic performance of the sonic crystal array.

The use of locally resonant scatterers has gained recent interest in the study of sonic crystals [1,2,6,7]. The result is the generation of locally resonant band gaps around the resonator natural frequency in addition to the band gap due to the overall periodicity of the sonic crystal array. Chalmers et al. [6] showed that the use of a C-shaped resonator is able to generate two bandgaps; one band gap due to the periodic arrangement of the scatterers and a second band gap attributed to resonance of the air inside the resonators. The band gap can be broadened using resonators of varying sizes. Elford et al. [7] considered multi-resonant scatterers for which C-shaped resonators of increasing size were arranged concentrically around each other in a Russian doll, or Matryoshka, format. The local resonance of each slotted resonator created transmission loss that was dependent only on the dimensions of the resonator cavity and unrelated to the periodicity of the sonic crystal.

In this work, the acoustic performance of a sonic crystal noise barrier using vertical cylindrical shells of finite height is numerically investigated. The insertion loss of the sonic crystal barrier obtained using either uniform or perforated cylindrical shell scatterers are compared. The effects of the number and size of the perforations on the barrier insertion loss is examined.

2. Numerical Model

A finite element (FE) model of the noise barrier was developed using COMSOL Multiphysics (v4.3b) [8]. The Helmholtz wave equation is solved for the acoustic pressure p at each frequency and is given by

$$\Delta p(\mathbf{x}) + k^2 p(\mathbf{x}) = 0 \tag{1}$$

where Δ is the Laplacian operator, k is the acoustic wavenumber and $\mathbf{x}$ is a point in the acoustic domain. The acoustic pressure in a discretised domain is given by

$$p(\mathbf{x}) = \sum_{i=1}^{N} \Phi_i(\mathbf{x})\, p_i \tag{2}$$

where p_i corresponds to the discrete acoustic pressure at point $\mathbf{x}$. $\Phi_i(\mathbf{x})$ are basis functions [9]. Substituting equation (2) into equation (1), applying non-reflecting boundary conditions and rearranging the resulting equations into one matrix equation yields [9]

$$(\mathbf{K} - jk\mathbf{C} - k^2\mathbf{M})\mathbf{p} = \mathbf{p}_i \tag{3}$$

where $\mathbf{K}$, $\mathbf{C}$ and $\mathbf{M}$ are the stiffness, damping and mass matrices, respectively, and $j = \sqrt{-1}$ is the imaginary number. The matrices $\mathbf{K}$ and $\mathbf{M}$ result directly from the integration of the basis functions while the matrix $\mathbf{C}$ represents the effects of the non-reflecting boundary conditions. The excitation vector $\mathbf{p}_i$ represents the incident pressure field and the vector $\mathbf{p}$ represents the acoustic pressure at the nodal locations in the acoustic domain.

3. Uniform and Perforated Cylindrical Shells

A numerical model of a periodic array of acoustically rigid uniform cylindrical shells was developed as follows. Three cylindrical shell scatterers in the *y*-direction were considered, as shown in Figure 1. A periodic boundary condition was applied in the *x*-direction of the domain to reduce the computational cost required to solve the finite element model, thus extending the length of the barrier to infinity in the positive and negative *x*-directions. A radiation boundary condition with an incident plane wave source of 1 Pa was applied to the left boundary. The plane wave source was located at a distance of 1 m from the mid-plane of the first row of cylinders. The receiver was located on the right face of the domain boundary in the barrier shadow zone. A rigid boundary condition was applied on the ground as well as the top surface of the domain, thereby neglecting diffraction over the top edge of the scatterers. The uniform cylindrical shells were then replaced with perforated cylindrical shells shown in Figure 2. The cylindrical shell scatterers have dimensions of height of h=3m, radius of the internal cylinder of r_1=0.18m, radius of the external cylinder of r_2=0.2m and cylindrical shell thickness of 20mm.

The lattice constant a is defined as the distance between the centres of adjacent scatterers and the filling fraction is defined as the ratio of the volume occupied by the scattering material with respect to the total volume of the sonic crystal. The centre frequency f_c of the band gap produced by the periodic array can be approximately predicted by Bragg's law and is given by

$$f_c = \frac{nc}{2a}, \quad n = 1, 2, 3, \ldots \tag{4}$$

where c is the speed of sound in the host medium which in this case is air. For the dimensions of the cylindrical shell scatterers considered in this work, the lattice constant is $a = 0.6$ m and the filling fraction is 0.35.

Sound attenuation by the sonic crystal noise barrier is expressed in terms of insertion loss (IL) as follows

$$\mathrm{IL} = \mathrm{SPL}_{\mathrm{without\ SC}} - \mathrm{SPL}_{\mathrm{with\ SC}} \tag{5}$$

where $\mathrm{SPL}_{\mathrm{without\ SC}}$ and $\mathrm{SPL}_{\mathrm{with\ SC}}$ are the sound pressure levels for the same receiver position without and with the noise barrier, respectively.

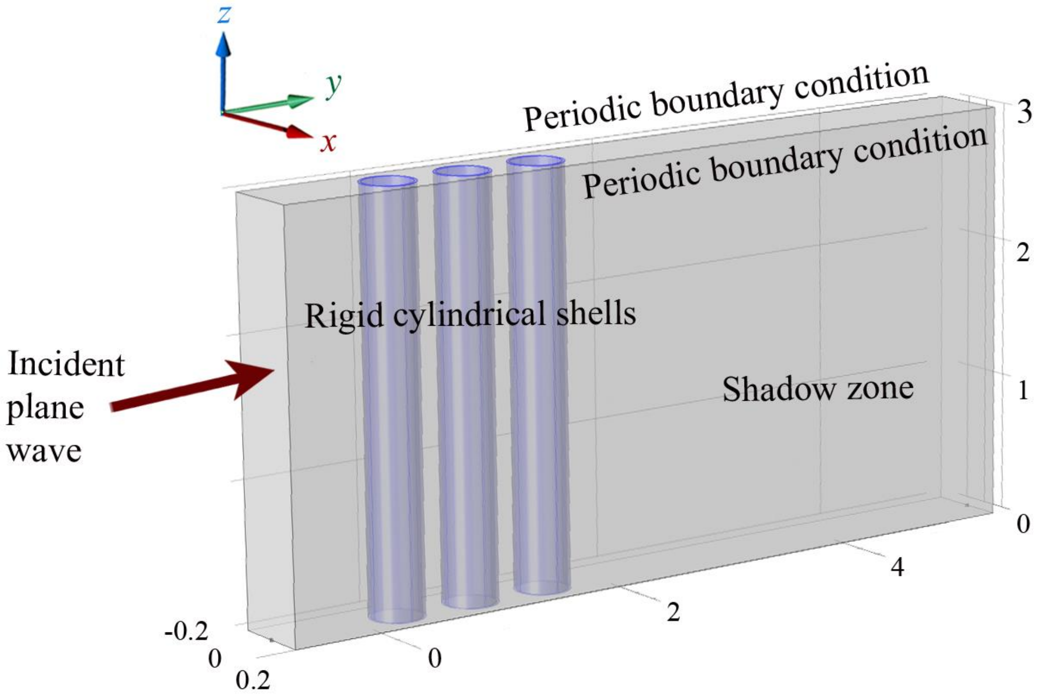

Figure 1. Configuration of the sonic crystal barrier showing the boundary conditions

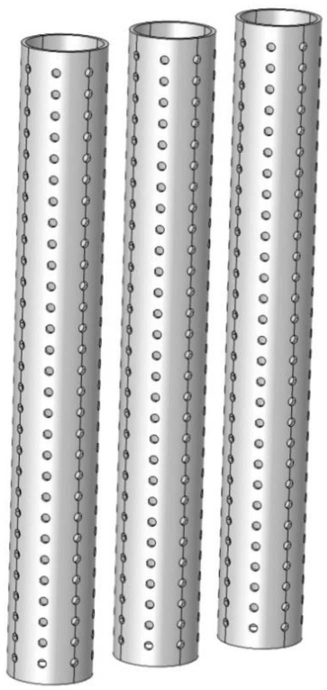

Figure 2. Schematic diagram of the rigid perforated cylindrical shells

4. Results

The insertion loss for a sonic crystal barrier using either uniform or perforated rigid cylindrical shells is presented in Figure 3. The perforated cylindrical shell scatterer has 8 holes around its circumference and 16 holes along its length, corresponding to a total of 128 holes. The radius of the holes is 20 mm. Using uniform cylindrical shell scatterers, a broad band gap is generated, attributed to destructive interference between reflected and scattered waves within the periodic array of cylinders. Peak insertion loss occurs around 270 Hz. The centre frequency of the band gap is also predicted using equation (4) for the first Bragg band gap, corresponding to 283 Hz for $c = 340$ m/s and lattice constant $a = 0.6$ m. For the sonic crystal barrier using perforated cylindrical shells, a narrow band peak in insertion loss is generated in addition to the broad band gap due to Bragg scattering. The frequency at which peak insertion loss occurs due to the locally resonant scatterers is independent of the periodicity of the sonic crystal array and instead can be approximately calculated by the natural frequency of a Helmholtz resonator which is given by

$$f_{\mathrm{HR}} = \frac{c}{2\pi}\sqrt{\frac{nS}{l'V}} \tag{6}$$

In equation (6), n is the total number of holes per cylindrical shell scatterer, S is the cross-sectional area of each hole and l' is the effective length of the neck of each hole. V is the volume of air in the cylindrical shell scatterer and is equal to $\pi r_1^2 h$, where r_1 is the radius of the internal cylinder and h is the cylinder height. The effective length l' is used to account for the fact that some extra volume of air around the neck moves with the air inside the neck and is given by

$$l' = l_n + Cr_h \tag{7}$$

l_n is the actual length of the neck of each hole, r_h is the radius of the holes and C is an empirically determined correction factor which is dependent on the geometry of the resonator. Here, the correction factor was found to be a linear function of the total surface area of the holes and is given by

$$C = -4.59nS + 1.42 \tag{8}$$

where $S = \pi r_h^2$ and the coefficients –4.59 and 1.42 are attributed to the size and number of the holes. According to equation (6), a lower resonant frequency can be achieved by increasing the internal volume of air in the cylindrical shell, increasing the length of the neck by increasing the thickness of the cylinder, or reducing the total surface area of the holes by either reducing the number of holes or reducing the radius of the holes. In Figure 3, the global increase in insertion loss of the Bragg band gap using perforated cylindrical shells is attributed to the Helmholtz resonator frequency associated with the narrow band peak insertion loss occurring within the frequency band gap due to the Bragg scattering.

The effect of hole radius of the perforated cylindrical shells on the barrier insertion loss is presented in Figure 4. Each perforated cylindrical shell scatterer has 8 holes around its circumference and 16 holes along its length. Decreasing the hole radius from 20 mm to 10 mm results in a decrease in the frequency at which the narrow band peak insertion loss occurs. As per equation (6), decreasing the hole radius results in a decrease in the total cross sectional area of the holes and hence a decrease in the resonant frequency. Since the resonant frequency due to the perforations no longer occurs within the band gap due to the Bragg scattering, the insertion loss due to the periodicity of the cylinders is now mostly unaffected by the locally resonant scatterers. When the hole radius is significantly increased to 40 mm, the perforated cylindrical shells no longer act as a sonic crystal, attributed to the fact that air can easily pass through the holes.

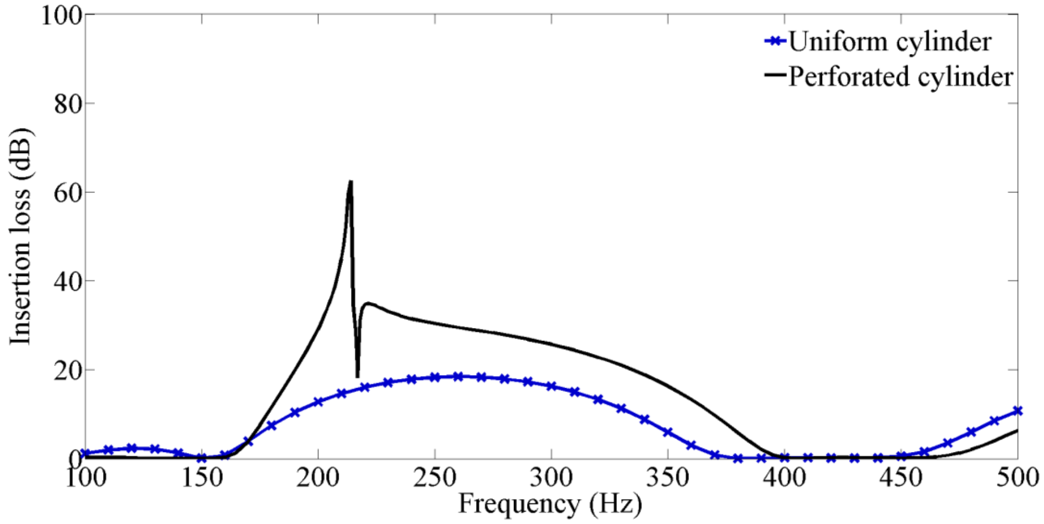

Figure 3. Insertion loss for a sonic crystal barrier using uniform or perforated rigid cylindrical shells

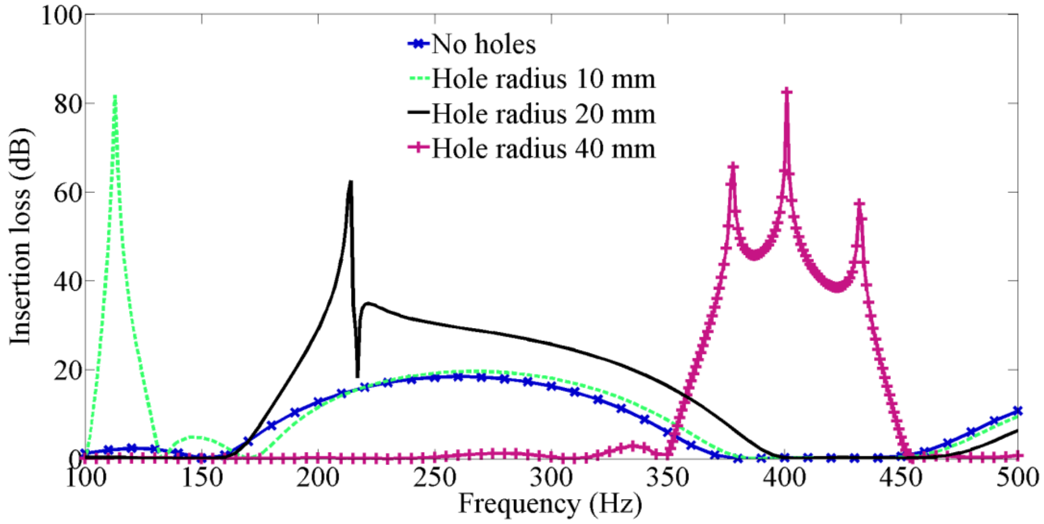

Figure 4. Insertion loss for a sonic crystal barrier using uniform cylindrical shells or perforated cylindrical shells with varying hole radius

Figure 5 illustrates the effect of varying the number of holes around the circumference of the perforated cylindrical shells on the insertion loss. The location of each resonant frequency is dependent on the number and size of the holes and independent of the periodic arrangement of the scatterers. Decreasing the number of holes results in a shift of peak insertion loss with higher attenuation to lower frequencies. This is attributed to the fact that the total surface area occupied by the holes has decreased. Increasing the number of holes around the circumference results in higher insertion loss at frequencies within the Bragg band gap due to the resonant frequency of the locally resonant scatterers occurring within the frequency band gap due to Bragg scattering.

The effect of the total number of holes on the insertion loss is now examined. In Figure 6, results are presented for which the number of holes around the circumference of the perforated cylindrical shell is halved (4 holes around the circumference, 16 holes along the length resulting in a total of 64 holes), or the number of holes along the length is halved (8 holes around the circumference, 8 holes along the length resulting in a total of 64 holes). By halving the number of holes either along the length or around the circumference, the resonant peak is shifted to lower frequencies due to a reduction in the total surface area occupied by the holes. Since the total surface area occupied by the holes is the same for both cases at which the number of holes is reduced, the frequency at which peak insertion loss occurs is unaffected.

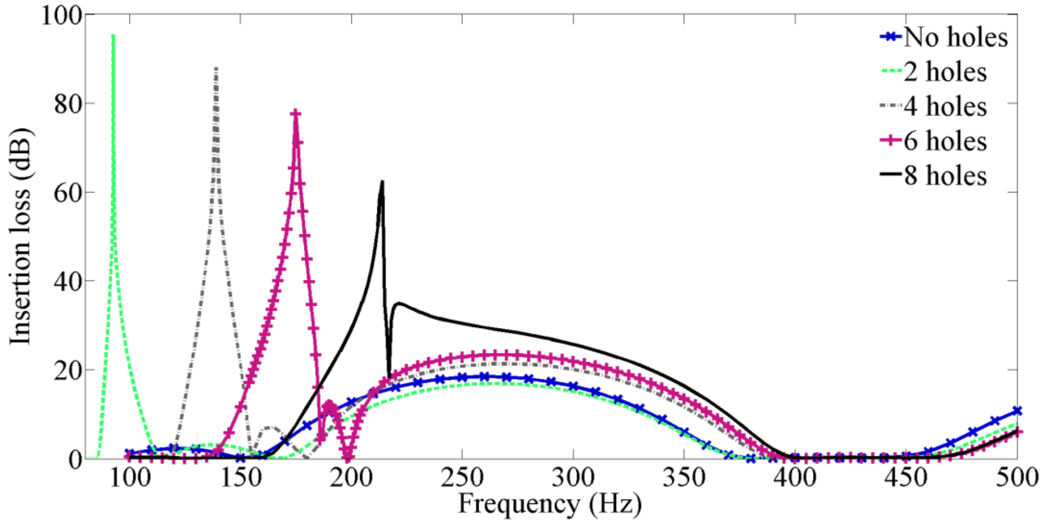

Figure 5. Insertion loss for a sonic crystal barrier using uniform cylindrical shells or perforated cylindrical shells with varying number of holes around the circumference

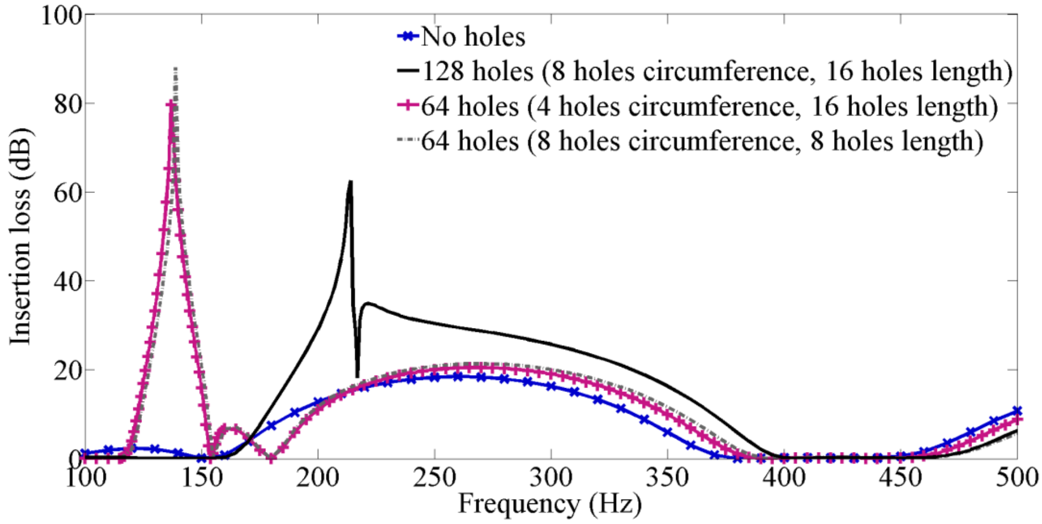

Figure 6. Insertion loss for a sonic crystal barrier using uniform cylindrical shells or perforated cylindrical shells with varying number of holes

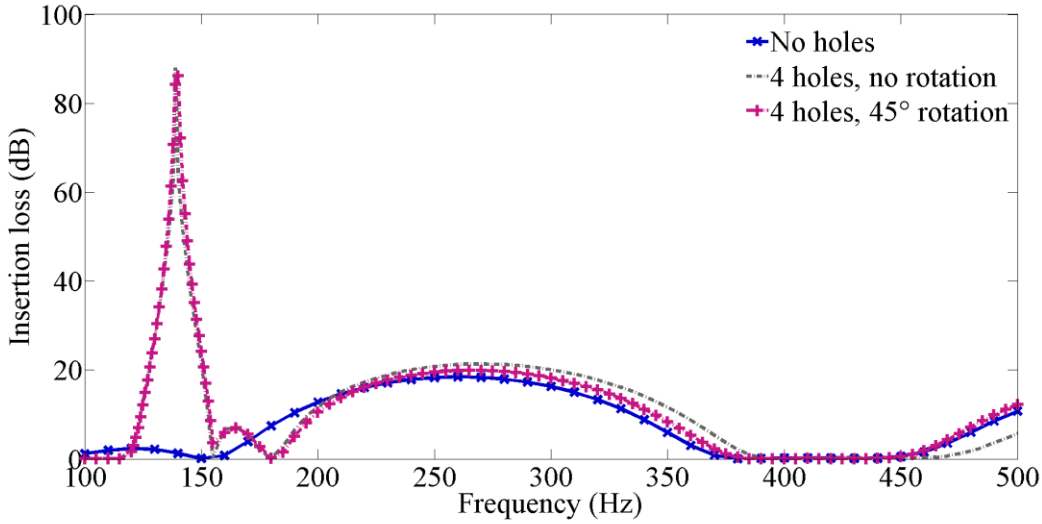

Figure 7. Insertion loss for a rigid perforated cylindrical shell sonic crystal barrier with varying number of holes around the circumference

The effect of rotating the location of the holes around the circumference of the perforated cylindrical shells is shown in Figure 7, using 4 holes around the circumference and 16 holes along the length such that the peak insertion loss at the Helmholtz resonator frequency is below the Bragg band gap. The location of the holes is then rotated by 45^{o} around the circumference. The results in this figure confirm those in Figure 6 in that the location of the holes does not affect the resonant frequency due to the perforations.

5. Summary

The acoustic performance of sonic crystal noise barriers comprising of uniform or perforated rigid cylindrical shells has been investigated. A Bragg band gap was generated due to the periodic arrangement of the cylindrical shell scatterers, dependent on the distance between the scatterers and the volume occupied by the scatterers. The local resonance of the perforated cylindrical shell scatterers created an additional peak in insertion loss, approximately predicted by the resonant frequency of a Helmholtz resonator. The location of the resonant frequency was shown to be dependent on the number and size of the holes and independent on the location of the holes. When the resonant frequency due to the perforations occurred within the Bragg band gap, a significant increase in insertion loss across the band gap was found to occur.

Acknowledgement

The financial assistance provided to the first author by Australian Acoustical Society NSW Division to attend the Acoustics 2015 Hunter Valley conference is gratefully acknowledged.

References

[1] Koussa, F., Defrance, J., Jean P. and Blanc-Benon. P. “Acoustical efficiency of a sonic crystal assisted noise barrier”, *Acta Acustica united with Acustica*, **99**, 399-409, (2013).

[2] Martins, M., Godinho, L. and Picado-Santos, L. “Numerical evaluation of sound attenuation provided by periodic structures”, *Archives of Acoustics*, **38**(4), 503-516 (2013).

[3] Krynkin, A., Umnova, O. Sánchez-Pérez, J.V., Chong, A.Y.B., Taherzadeh S. and Attenborough, K. “Acoustic insertion loss due to two dimensional periodic arrays of circular cylinders parallel to a nearby surface”, *Journal of the Acoustical Society of America*, **130**(6), 3736-3745, (2011).

[4] Sanchez-Dehesa, J., Garcia-Chocano, V. M., Torrent, D., Cervera, F. and Cabrera, S. “Noise control by sonic crystal barriers made of recycled materials”, *Journal of the Acoustical Society of America*, **129**(3), 1173-1183, (2011).

[5] Kessissoglou, N., Fard, S.M.B., Keightley, T., Peters H. and Marburg. S. “Acoustic performance of sonic crystal noise barriers using a quasi-periodic boundary element technique”, *Noise and Vibrations – Emerging Technologies*, Dubrovnik, Croatia, 13-15 April 2015.

[6] Chalmers, L., Elford, D.P., Kusmartsev, F.V. and Swallowe, G.M. “Acoustic band gap formation in two-dimensional locally resonant sonic crystals comprised of Helmholtz resonators”, *International Journal of Modern Physics B*, **23**, 4234-4243, (2009).

[7] Elford, D.P., Chalmers, L., Kusmartsev, F.V. and Swallowe, G.M. “Matryoshka locally resonant sonic crystal”, *Journal of the Acoustical Society of America*, **130**, 2746-2755, (2011).

[8] COMSOL Multiphysics, Version 4.3b, 2013.

[9] Marburg, S. and Nolte, B. *Computational acoustics of noise propagation in fluids*, Chapter 0: A unified approach to finite and boundary element discretization in linear acoustics, Springer, Berlin, Germany, 2008, pp. 1-34.